

# Revisiting Reading Rate with Mobility: Rate-Adaptive Reading in COTS RFID Systems

Qiongzhen Lin<sup>\*†</sup>, Lei Yang<sup>\*</sup>, Huanyu Jia<sup>†</sup>, Chunhui Duan<sup>\*†</sup>, Yunhao Liu<sup>†</sup>

<sup>\*</sup>Department of Computing, The Hong Kong Polytechnic University

<sup>†</sup>School of Software, Tsinghua University

{young,lin,jia,hui}@tagsys.org,yunhao@greenorbs.com

## ABSTRACT

Radio-frequency identification (RFID) systems, as major enablers of automatic identification, are currently supplemented with various interesting sensing functions, *e.g.*, motion tracking. All these sensing applications forcedly require much higher reading rate (*i.e.*, sampling rate) such that any fast movement of tagged objects can be accurately captured in a timely manner through tag readings. However, COTS RFID systems suffer from an extremely low individual reading rate when multiple tags are present, due to their intense channel contention in the link layer. In this work, we present a holistic system, called Tagwatch, a rate-adaptive reading system for COTS RFID devices. This work revisits the reading rate from a distinctive perspective: *mobility*. We observe that the reading demands of mobile tags are considerably more urgent than those of stationary tags because the states of the latter nearly remain unchanged; meanwhile, only a few tags (*e.g.*, < 20%) are actually in motion despite the existence of a massive amount of tags in practice. Thus, Tagwatch adaptively improves the reading rates for mobile tags by cutting down the readings of stationary tags. Our main contribution is a two-phase reading design, wherein the mobile tags are discriminated in the Phase I and *exclusively* read in the Phase II. We built a prototype of Tagwatch with COTS RFID readers and tags. Results from our microbenchmark analysis demonstrate that the new design outperforms the reading rate by 3.2× when 5% of tags are moving.

## CCS CONCEPTS

• **Networks** → **Cyber-physical networks**; • **Computer systems organization** → **Embedded and cyber-physical systems**;

## KEYWORDS

RFID; Rate-Adaptive Reading; EPCGlobal Gen2; Two-phase Protocol; Tagwatch

---

Permission to make digital or hard copies of all or part of this work for personal or classroom use is granted without fee provided that copies are not made or distributed for profit or commercial advantage and that copies bear this notice and the full citation on the first page. Copyrights for components of this work owned by others than the author(s) must be honored. Abstracting with credit is permitted. To copy otherwise, or republish, to post on servers or to redistribute to lists, requires prior specific permission and/or a fee. Request permissions from [permissions@acm.org](mailto:permissions@acm.org).

CoNEXT '17, December 12–15, 2017, Incheon, Republic of Korea

© 2017 Copyright held by the owner/author(s). Publication rights licensed to Association for Computing Machinery.

ACM ISBN 978-1-4503-5422-6/17/12...\$15.00

<https://doi.org/10.1145/3143361.3143387>

## 1 INTRODUCTION

Radio-frequency identification (RFID), as one of the top 10 influential technologies in the 21st century [9], is widely used in various fields, such as logistic, supply chain management, asset management, and so on. In contrast to conventional identification technologies (*e.g.*, barcode), RFID offers many attractive advantages, such as non-optical proximity, long transmission range, multiple inventory, and so on. The initial purpose of RFID is to automatically identify (*i.e.*, Auto-ID) objects fast and conveniently. Its potential applications have been explored in the past decade; among which, the most promising is in tracking mobile objects. Many applications benefit from highly accurate motion tracking. For example, supermarkets can thoroughly observe the shopping habits of consumers by monitoring the trajectories of items [22]. Several new battery-free human-machine interactive devices can be developed, such as writing letters in the air by attaching a tag to a finger [27]. Complex multiplayer behavior is also automatically recognized through a tagged football in an international game [10]. Enabling a robot to search for, pick up, fetch, and deliver a particular object from an assembly line has received considerable interest in both the academic community and various industries [25]. High-precision 3D orientation [29] or rotations [31] of passive objects are monitored through backscatter signals from tags.

The basic concept behind the above tracking applications is to regard each tag reading as one sampling of its motion state (or state of its attached object), which imposes a tacit assumption; that is, the sampling rate (*i.e.*, reading rate, the number of reading times per second) must be sufficiently high, such that an object's state changes can be continuously and faultlessly captured using tag readings for both slow and fast transitions. To visually illustrate the impact of reading rate on motion tracking, Fig. 1(a) shows an example<sup>1</sup> in which the trajectory of a tagged toy train moving along a circular track is recovered. Moreover, we place two and four stationary tags beside the track. Consequently, the reading rate of the mobile tag is sharply reduced from 68Hz (*i.e.*, no stationary tag) to 30Hz (*i.e.*, two stationary tags) and 21Hz (*i.e.*, four stationary tags) due to the channel contentions in the link layer. Correspondingly, the mean tracking accuracy (for additional details including the tracking algorithm, see §7) decreases from 1.8cm to 10cm (*i.e.*, about 10× drop). Clearly, reading rate considerably affects motion surveillance, particularly when multiple tags are present.

A number of recent works have attempted to explore the possibility of improving reading rate from two layers. (1) The first group

<sup>1</sup>Despite a single moving tag shown in the example, our system can deal with the case where multiple mobile objects present.

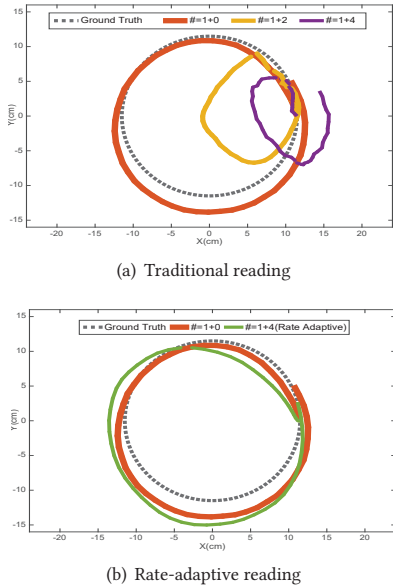


**Fig. 1: Tracing a mobile object using one RFID tag in company with different numbers of stationary tags. (a) Traditional reading with zero, two and four stationary tags. (b) Rate-adaptive reading with four stationary tags.**

of studies enables RFID tags to transmit in parallel in the physical layer [3, 12, 21, 26]. However, these work cannot be applied to mobile tags because they require tags remaining the channel coefficients relatively unchanged. Clearly, moving tags change their coefficients rapidly, making physical symbol clusters in the constellation domain difficult to distinguish. (2) The second group of studies attempts to design efficient anti-collision protocols. RFID tags respond completely to a centralized scheduling of a reader for medium access. The current inefficient scheduling mechanism has resulted in a large number of *useless* empty and collided slots. Prior designs [4, 7, 15, 17], however, require substantial modifications to COTS tags or reader to enable collision resolution. The aforementioned two types of schemes can hardly benefit from the existing deployment of billions of COTS RFID tags worldwide with globalized standards.

Unlike the above prior works, we explore tag’s reading rate from the third perspective: *mobility*. We observe that only a few tags (*e.g.*, < 20%) are actually in motion despite the existence of a massive amount of tags in practice. For example, tens out of thousands of goods in a supermarket or warehouse are simultaneously picked up by a customer in an instant. Our real trace data acquired from a medium-sized sorting system also suggest that less than 10% of package pieces are being transported on conveyors. The remaining package pieces are sorted well and always remain stationary. Stationary tags do not urgently require a high reading rate because their states remains unchanged (*i.e.*, similar to the state obtained in the previous time). Therefore, we should treat the individual reading rate for each tag differently and perform a *rate-adaptive*

*reading*, which allocates more time for reading mobile tags but less time for reading static tags.

In this work, we present a holistic system, called Tagwatch, a rate-adaptive reading system for COTS RFID devices. This system offers higher reading rate for mobile tags, which have high priority in surveillance applications. Transforming this high-level idea into a practical system requires addressing two main challenges. (1) *How do we know which tags are moving?* Identifying mobile tags is challenging because their movements are unpredictable, particularly in a rapidly changing environment with non-ideal communication conditions. Even worse, a static tag may suddenly start to move at any time, or vice versa. (2) *How do we exclusively read a specific set of mobile tags without reading stationary tags?* The naive solution of dividing space for multiple access fails because the spatial distribution of mobile tags are totally unknown, and the mobile tags may frequently go across multiple divisions. Inappropriate space division may lead to massive unexpected readings of stationary tags, which are collaterally covered.

To address these challenging issues, Tagwatch adopts a two-phase reading design. In the first phase, Tagwatch begins a relatively shorter inventory procedure to read all tags. Thereafter, Tagwatch performs a motion assessment using backscatter signals from tags to identify mobile tags (see §4). In the second phase, Tagwatch performs selective reading (*i.e.*, using `Select` command), to intensively and exclusively read mobile tags for a relatively longer interval (see §5). In this manner, the average individual reading rates of mobile tags are significantly increased. Fig. 1(b) shows the recovered trajectory of a mobile tag in company with four interfered stationary tags using rate-adaptive reading. Even with the presence of four other tags, the mean accuracy (*i.e.*, 3.34cm) of the recovered trajectory remains as good as that obtained without a static tag.

**Summary of Results:** Tagwatch works with COTS RFID devices and is a purely software solution. We built and evaluated a prototype of Tagwatch using ImpinJ readers and numerous Alien tags (see §6). We conducted extensive testbed experiments in our laboratory (see §7) and obtained the following findings:

- We accurately model the reading rate for current COTS readers. Both the model and our empirical study indicate that the mean individual reading rate will drastically decrease by 84% when the total number of tags is over 30.
- Tagwatch can successfully identify mobile tags with a mean probability of 80% as long as a tag moves beyond 1cm. It also achieves 95% of accuracy for motion detection, whereas the false positive rate (FPR) is maintained at below 10%.
- Tagwatch can outperform the individual reading rates of mobile tags by a median of 3.2× and 1.9× when there are 5% and 10% mobile tags.

**Contributions.** In this work, we made the following contributions: To the best of our knowledge, Tagwatch is the first RFID system that performs rate-adaptive reading on COTS devices by considering tag’s mobility. It solves a practical problem in the domain of motion surveillance using RFID tags. Specifically, we introduce the algorithm of motion assessment to automatically identify mobile tags without an ideal communication model. Second, by converting selective reading into the set-covering problem, we

present a scheduling algorithm for the selective reading of mobile tags. Third, we systematically evaluate the system.

## 2 BACKGROUND & MOTIVATION

This section reviews the background of RFID inventory, presents the theoretical model of reading rate, and then shows the motivation behind the rate-adaptive reading.

### 2.1 Reading Rate: State-of-the-Art

RFID systems adopt the reader-talks-first mode, in which the reader dominates communication and all the tags follow its commands. The Individual Reading Rates (IRR) of tags, defined as the number of readings obtained from a particular tag per second, highly depend on the efficiency of the anti-collision protocol, which is used to avoid signal collisions that occur when multiple tags reply their IDs simultaneously. Subsequently, we gradually introduce the anti-collision protocol used in COTS RFID systems.

**Framed Slotted ALOHA(FSA).** FSA is the basic anti-collision protocol. In FSA, the reader divides time into several slots, which are further organized into frames. The reader broadcasts the `Select` command to start an inventory round, which consists of several frames. In the beginning of a frame, the reader broadcasts the command `Query` which takes the parameter of the frame length  $f$  (i.e., the number of slots present in the current frame). After receiving the `Query` command, each tag randomly selects an integer  $\in [0, f - 1]$  and stores it in the local variable `SC`. Afterwards, the reader starts a time slot by broadcasting `QueryRep`, which lets the tag decrease its `SC` by one. If the `SC` of the tag is equal to 0, then it immediately replies with a 16-bit random signal (i.e., RN16). The tag that chooses a collision-free slot is acknowledged with the `ACK` command and allowed to transmit its EPC in the subsequent time slice. Otherwise, the reader sends `QueryRep` to proceed to the next time slot. This process continues until collision is no longer detected.

**Q-Adaptive.** The probability that a given time slot of FSA will make a single reply, denoted by  $q$ , is given by

$$q = \binom{n}{1} \frac{1}{f} \left(1 - \frac{1}{f}\right)^{n-1} \quad (1)$$

where  $n$  is the total number of tags. When the derivative of the preceding equation is taken, the maximum probability is obtained  $q_{\max} = 1/e$  where  $f = n$ . That is, to achieve the maximum reading rate, the frame length should always be set to the total number of tags participating in the current frame. The ideal FSA can be designed as follows. (1)  $f = n$  is initialized. (2) Each time a tag is successfully identified, the current frame is terminated and a new frame starts with  $f = f - 1$ , such that each slot maintains the maximum probability of a successful reply. The frame length is dynamically adjusted; hence, we call the scheme *Dynamic FSA* (DFSA). However, the reader does not have a *priori* knowledge about  $n$ . To address this issue, a COTS reader (i.e., aka Gen2 reader) adopts the Q-adaptive protocol, which can adaptively estimate  $n$  according to history readings, and is based on an *award-punish* mechanism. In particular, the command `Query` contains a non-negative integer  $Q$ , which indicates the frame length  $f = 2^Q$ . The reader dynamically increases or decreases  $Q$  at the end of each collided slot or empty slot.

### 2.2 Theoretical Analysis of Reading Rate

Assume that the frame length can always be adjusted to the optimal value. How much time will the reader consume in an inventory round? This question can be reduced into the classical *Coupon Collector's Problem*, which states that there are  $n$  distinct objects that are repeatedly drawn (with replacement) from an urn with a probability of  $1/n$  of picking an object at each trial. What is the minimum number of trials needed to pick each of the  $n$  objects at least once? We sketch the analysis as follows. When  $f = n$ , and thus, the probability that the  $i^{\text{th}}$  tag is successfully identified in a given slot is equal to:

$$p = \frac{1}{n} \left(1 - \frac{1}{n}\right)^{n-1} \approx \frac{1}{ne} \quad (2)$$

Let the random variable  $\mathcal{F}$  denote the number of slots required by the reader to collect  $n$  tags, and  $f_i$  denote the length of the  $i^{\text{th}}$  frame,  $0 \leq i \leq n-1$ , which starts when the  $i^{\text{th}}$  tag is identified and ends when the  $(i+1)^{\text{th}}$  tag is identified. Thus,  $n-i$  tags are yet to be read in the  $i^{\text{th}}$  frame, and each of these tags has a probability  $p$  of being read in a time slot. The frame length,  $f_i$ , is a geometric random variable with parameter  $(n-i)p$ . Thus, when  $\mathcal{F} = f_0 + \dots + f_{n-1}$ , we obtain

$$E[\mathcal{F}] = \sum_{i=0}^{n-1} E[f_i] = \sum_{i=0}^{n-1} \frac{1}{(n-i)p} = \frac{1}{p} \sum_{i=1}^n \frac{1}{i} = \frac{1}{p} H_n \approx ne H_n \quad (3)$$

where  $H_n$  denotes the  $n^{\text{th}}$  harmonic number and is given by  $\ln n + O(1)$ . Therefore,

$$E[\mathcal{F}] = ne(\ln n + O(1)) \approx ne \ln n + O(n) \quad (4)$$

$E[\mathcal{F}]$  approaches  $ne \ln n$  time slots for a large value of  $n$ , where each tag can be read once within  $ne \ln n$  slots.

In addition to the time for collecting tags, each inventory round will introduce an extra time cost for other necessary tasks, e.g., broadcasting `Select`, synchronization, and clearing history states. We call such time consumption as *start-up cost*, which is denoted by  $\tau_0$ . Suppose that the mean duration<sup>2</sup> of each slot is equal to  $\bar{\tau}$ , then the entire inventory cost is defined as follows:

**DEFINITION 1 (INVENTORY COST).** *Inventory cost, denoted by  $C(n)$ , is defined as the total time consumed on identifying  $n$  tags once. It is given by*

$$C(n) = \begin{cases} \tau_0 + ne\bar{\tau} \ln(n) & \text{if } n > 1 \\ \tau_0 + \bar{\tau} & \text{otherwise} \end{cases} \quad (5)$$

With regards to the inventory cost, IRR is then given by

$$\Lambda(n) = \frac{1}{\tau_0 + ne\bar{\tau} \ln(n)} \quad (6)$$

This equation provides a fundamental estimation model for calculating the scheduling cost (later used in §5). To the best of our knowledge, we are the first to *accurately* model the IRR for COTS RFID system, particularly the impact of start-cost, which was never considered before. Next, we conduct empirical experiments to validate its correctness.

<sup>2</sup>The actual successful slot is longer than empty and collided slots due to the transmission of EPC. Thus, we use an average approximation.

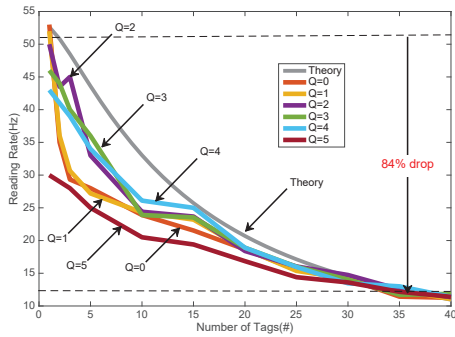


**Fig. 2: Empirical study on IRR.** Gen2 protocol allows upper application to set an initial  $Q$  as figure shows. However, the reader will gradually and automatically adjust the actual  $Q$ , making total inventory time approach optimal.

### 2.3 Empirical Analysis of Reading Rate

We then practically measure the reading rates of the ImpinJ R420 reader across 1 ~ 40 Alien tags, with various frequencies (920 ~ 926MHz), including 16 channels. We try different initial settings of  $Q$  in the experiments. For each setting, we repeat the experiment 50 times and report the average value. We also utilize the least-squares algorithm to estimate the two unknown parameters, namely,  $\tau_0$  (19ms) and  $\bar{\tau}$  (0.18ms), involved in Eqn. 6. The average IRR is depicted in Fig. 2. The following two findings are obtained from the studies:

(1) Our theoretical formula for IRR agrees well with the measurement results in terms of the trend, except for a slight difference due to the approximation in Eqn. 4. This indicates that the current anti-collision algorithm, *i.e.*,  $Q$ -adaptive, is already a good algorithm approaching the optimal solution. Thus, current system leaves very limited room to improve the reading rate by designing better anti-collision protocols.

(2) IRR is a purely decreasing function of  $n$ , *i.e.*, inversely proportional to  $n \ln(n)$ . Specifically, as shown in Fig. 2, IRR decreases from 63Hz to 12Hz (*i.e.*, an 84% drop) when  $n$  increases to near 40. This finding hints that companionate tags would seriously and negatively affect the IRRs of the tags of interest.

### 2.4 Motivation

We consider the issue of reading rate in real situations where billions of COTS RFID tags have been deployed and covered by RFID readers. We can neither change the device settings nor improve the efficiency of the current anti-collision protocol. We are not allowed to communicate tags with different frequency channels simultaneously (so that reading some tags more faster at one pace and the others at a slower pace), because tags do not equip with transceivers and must backscatter their IDs using the same frequency as emitted by the reader. In short, there is no way to apply frequency division multiple access (*i.e.*, FDMA) in current RFID systems. With such rigorous rules, how can we improve the IRR of mobile tags?

**Case study.** We collect a real reading trace from our previous tracking system, TrackPoint [30], *i.e.*, a gate composed of three

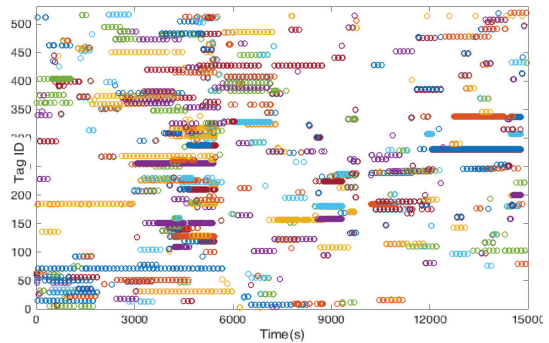


**Fig. 3: Reading trace.** An approximately 4 hour real trace acquired by the TrackPoint in which our RFID reader obtained up to 367, 536 readings from 527 tags.

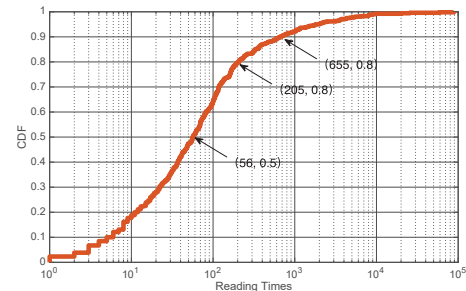


**Fig. 4: Trace distribution.** We find that 20% of the tags are read over 205 times, whereas 10% of the tags are read over 655 times. In fact, each individual tag is supposed to be read about 50 times when it passes through the TrackPoint.

reader antennas is mounted above the conveyor to monitor moving baggage. We expect that each tag can be read 10 times *immediately during* it is moved through the device, so as to localize each baggage at a high-precision level. We choose an approximately 4 hour real trace, as shown in Fig. 3, during which our RFID reader obtained up to 367, 536 readings from 527 tags. We visually observe that 30 tags ( $\approx 5.7\%$  tags) at most are simultaneously conveyed through the TrackPoint each second. However, Tag #271 has been continuously read 90,000 times, in that the corresponding tagged package was placed on the side of the vehicle near to the TrackPoint; it actually stays there without moving. Obviously, the readings of tag #271 are unwanted. Furthermore, we also show the distribution of reading times in Fig. 4. We find that 20% of the tags are read over 205 times, whereas 10% of the tags are read over 655 times. In fact, each individual tag should be read about 50 times when it passes through the gate. All these exceptional readings come from these tags, which are actually not moved on the conveyor but have been sorted and stayed nearby TrackPoints. By contrast, the real moving tags are typically read less than 5 times when being moved across the gate, due to the channel contentions from nearby stationary tags.



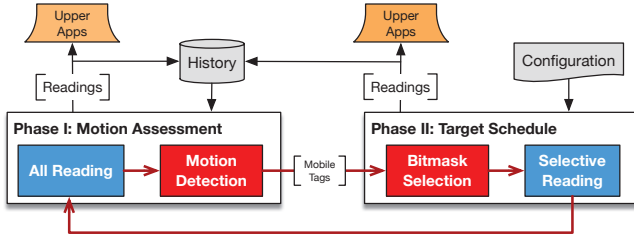


**Fig. 5: System architecture.** Tagwatch adopts a two-phase reading design, wherein the motion state of each tag is assessed in the first phase and only moving tags are read in the second phase.

In summary, our empirical data suggests that only a few number of tags from a massive number of tags (e.g., 10%) are concurrently moving in practice, and their reading demand are urgent. Meanwhile, The IRRs of moving tags are seriously affected by the nearby static tags. Thus, reducing the total number of participating tags in the inventory is a good way of improving the IRR of mobile tags. This inspire us to revisit IRR from the perspective of mobility: *real-time adjustment of the IRR according to tag’s current motion state.*

### 3 OVERVIEW

Tagwatch is a middle layer that runs between the reader and upper applications. It aims to *adaptively* change the reading rate of tags in terms of their motion states. As shown in Fig. 5, Tagwatch adopts a two-phase reading design:

**Phase I: Motion assessment.** In this phase, Tagwatch reads *all tags* within a short period and then leverages the reading results to assess the motion state of each tag. Afterwards, Tagwatch selects *mobile tags* to be scheduled in the next phase according to the history-based immobility models.

**Phase II: Target schedule.** In this phase, Tagwatch first selects a group of bitmasks to cover target tags (e.g., mobile tags) and then conducts bitmask-enabled selective reading on target tags for a relatively long period.

The two phases constitute a basic cycle, which occurs alternatively and periodically as shown in Fig. 6. The scheduling phase is longer than the assessment phase, which guarantees target tags gain sufficient time to be read for several cycles. A periodical motion assessment is necessary to capture the state transitions of tags (e.g., from a moving state to a static state, or vice versa). Target tags are read for a longer period, and thus, their average IRRs are higher than those of other tags. Regardless of the phase in which tags are read, all readings should be delivered to upper applications and contribute to the history database.

**Scope.** Our system is driven by the assumption that quite small percent of tags are moving in a moment. It is possible that Tagwatch cannot obviously improve IRRs for mobile tags if the percent is over than a threshold (e.g., > 20%). Keep in mind that as our baseline is to read all tags, it is easy for us to switch back to the old fashion (i.e., reading them all) when the assumption does not hold true.

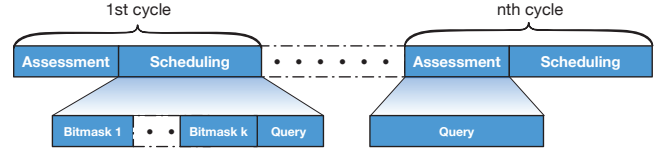


**Fig. 6: Reading cycles.** Each reading cycle is composed of two phase and occurs alternatively and periodically.

## 4 PHASE I: MOTION ASSESSMENT

This section discusses the first phase, wherein all the tags are continuously read once. The purpose of this phase is to identify all mobile tags.

### 4.1 Modeling Tag’s Immobility

To determine which tags are moving, we utilize the physical RF signals of tags. The reading result of a tag contains two basic physical metrics, RF strength and phase. Most COTS RFID systems support milli-degree resolution in detecting RF phase (i.e., hypersensitive to the movement of the tag), thus, we adopt the RF phase as a main measurement for motion detection.

**Challenges.** The naive method of perceiving the motion of a tag is to compare its incoming RF phase with the last one. If the two phases are same, then the tag is determined to be static; otherwise, it is in motion. However, such method suffers from a high rate of false positives because of the following reasons. (1) The phase estimate is derived from the received signal where the thermal noise from reader receiver is always present, thereby leading to measurement errors. (2) The RF signal propagation does not only occur along the direct path, i.e., line of sight (LOS), but also reflected by surrounding objects (particularly mobile objects). This phenomenon is known as the multipath effect. The final signal received at the receiver is a superposition of multiple copies of the original signals from all paths. Even if the original tag remains stationary, the movements of surrounding objects will create or cancel multipath propositions, thereby resulting in significant jumps of the RF phase.

**Gaussian model.** A number of prior empirical works [30, 32] have shown that the RF phase measurement results contain random errors, following a typical Gaussian distribution. Thus, we consider the phase measurement for each tag in the scene as a Gaussian random variable instead of an accurate value. Assume that we currently have the  $m$  RF phase values, i.e.,  $\{\theta_1, \theta_2, \dots, \theta_m\}$  for a particular tag. Then the incoming new phase  $\theta_{m+1}$  should follow a Gaussian model, i.e.,

$$\theta_{m+1} \sim \mathcal{N}(\mu_m, \delta_m) \quad (7)$$

where  $\mu_m$  and  $\delta_m$  are the expectation and the standard deviation that estimated through the history readings as follows.

$$\mu_m = \frac{1}{m} \sum_{i=1}^m \theta_i \text{ and } \delta_m = \sqrt{\frac{1}{m} \sum_{i=1}^m (\theta_i - \mu_m)^2} \quad (8)$$

If the tag’s position remains unchanged, the incoming RF phase  $\theta_{m+1}$  should follow the above Gaussian model, whose probability

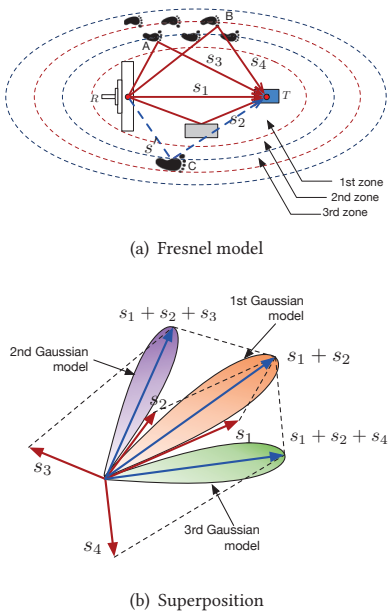


**Fig. 7: Mixed Gaussian model.** (a) An example showing how a surrounding mobile object affects the final RF signal. (b) The final RF signal received by the reader in three cases.

density function is given by

$$\eta(\theta_m, \mu_m, \delta_m) = \frac{1}{\delta_m \sqrt{2\pi}} \exp\left(-\frac{(\theta_m - \mu_m)^2}{2\delta_m^2}\right) \quad (9)$$

Initially, we assume all the tags are in motion (*i.e.*,  $\mu_0 = 0$  and  $\theta_0 = 0$ ) and then immediately learn their immobility. Correspondingly, a tag is static if the incoming phase value matches the Gaussian model, *i.e.*,  $|\theta_{m+1} - \mu_m| < \xi \delta_m$  where  $\xi$  is a user-defined parameter.

**Gaussian Mixture Model (GMM).** RF phase is known for its sensitivity to the motion of a tag but notorious for being too excessively sensitive to the movements of surrounding objects due to the multipath effect. Fig. 7(a) illustrates a toy example in which a person walks by a pair of reader and tag. Two constant signal propagations are available:  $s_1$  and  $s_2$ . By default, the final signal received by the reader is  $s_1 + s_2$ , as shown in Fig. 7(b). When the person passes by position A and B, he/she respectively introduces two new propagations,  $s_3$  and  $s_4$ , causing the final signal to jump from  $s_1 + s_2$  to  $s_1 + s_2 + s_3$  and  $s_1 + s_2 + s_4$ . Evidently, single Gaussian model fails to depict such jumps, producing two false positives.

We can divide a space into many Fresnel zones for every  $\lambda/2$  given a wavelength of  $\lambda$ , as shown in Fig. 7(a). Let R and T be a pair of reader and tag. The Fresnel zones contains  $K$  ellipses can be constructed as follows:

$$|RQ_k| + |Q_kT| - |RT| = k\lambda/2 \quad (10)$$

where  $Q_k$  is a point on the  $k^{th}$  ellipse. The preceding equation indicates the distance from points on the ellipse to two foci is  $k\lambda/2$  longer than the distance between the transmitter and receiver. The innermost ellipse is defined as the first Fresnel zone, and the  $k^{th}$  Fresnel zone corresponds to the elliptical annuli between the

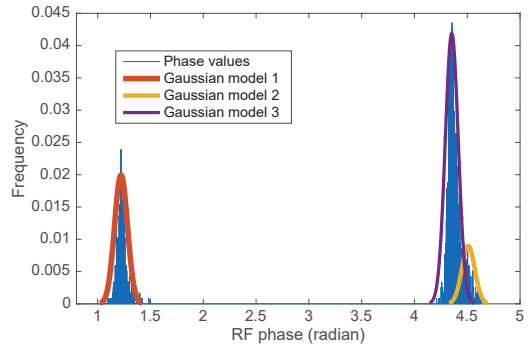


**Fig. 8: Use of GMM to model the immobility of a tag.**

$(k-1)^{th}$  and the  $k^{th}$  ellipse. Clearly, the reflections caused by the objects located at odd zones superimposes LOS signal in phase, whereas the superpositions with reflections from even zones are out of phase. The previous research [11, 24] shows that the significant zones for RF transmission are the first 3 ~ 8 zones, more than 70% of the energy is transferred via the first Fresnel zone.

The Fresnel zone model<sup>3</sup> inspires us to re-build the immobility of a tag using multiple Gaussian models, *i.e.*, Gaussian mixture model (GMM), wherein each combined propagation (*i.e.*, multipath) result corresponds to a Gaussian model. As shown in Fig. 7(b), three Gaussian models exist for the RF phase:  $\angle(s_1 + s_2)$ ,  $\angle(s_1 + s_2 + s_3)$  and  $\angle(s_1 + s_2 + s_4)$ . Fig. 8 shows the distribution of the phase values collected from a stationary tag in a dynamic environment (*i.e.*, asking a person to work around). The value of the RF phase follows a group of Gaussians models instead of a single model. In particular, suppose we have learned  $K$  Gaussian models, denoted by  $\{\mathcal{N}_1(\mu_1, m, \delta_1, m), \dots, \mathcal{N}_K(\mu_K, m, \delta_K, m)\}$ , for a particular stationary tag. During detection, the best matched Gaussian model (*e.g.*,  $k'$ -th) is chosen to depict the current immobility of a tag. The determining rule is thereby updated to  $|\theta_{m+1} - \mu_{k', m}| < \xi \delta_{k', m}$ .

## 4.2 Self-learning Motion Detection

Self-learning motion detection based on GMM is illustrated. First,  $K$  Gaussian models are assigned an initial large deviation  $\delta_k$  and low prior weight  $w_k$ . These  $K$  Gaussian models are ordered by the priority of  $r_k = w_k/\delta_k$ , because a Gaussian model with a high weight but a small deviation is preferred. The Gaussian model with the lowest priority will be gradually eliminated.

**Algorithm.** We build a stack of Gaussian models for each tag independently. On the incoming reading, a new RF phase value  $\theta_{m+1}$  is provided. The Gaussian model is “matched” if  $\theta_{m+1}$  is within  $\xi \times$  standard deviation of the Gaussian model, *i.e.*,  $|\theta_{m+1} - \mu_k| < \xi \delta_k$ . We search for the first matched model from top to down in terms of priority. Then one of the following two cases is observed:

- **Case 1:** If a match is found with one of the  $K$  Gaussian models in the stack, then the tag is classified as stationary. Correspondingly, we increase the weight of this model, adjust its mean closer

<sup>3</sup>Note we apply Fresnel theory to *explain* why we use GMM to build the immobility of a tag. Finding Fresnel zones is unnecessary because our detection algorithm is self-learning and adaptive to changes in the environment.

to  $\theta_{m+1}$ , and decrease the variance as follows:

$$\begin{cases} w_{k,m+1} = (1 - \alpha) \times w_{k,m} + \alpha \\ \mu_{k,m+1} = (1 - \rho)\mu_{k,m} + \rho\theta_{m+1} \\ \delta_{k,m+1} = \sqrt{(1 - \rho)\delta_{k,m}^2 + \rho(\theta_{m+1} - \mu_{m+1})^2} \end{cases} \quad (11)$$

where  $\alpha$  is a learning rate and  $\rho = \alpha\eta(\theta_{m+1}, \mu_m, \delta_n)^4$ . For the unmatched models, we maintain their mean and deviation, but decrease their weights to  $w_{k,m+1} = (1 - \alpha)w_{k,m}$ .

- **Case 2:** A match is not found with any of the  $K$  Gaussian models. In this case, the tag is classified as being in motion. A new model with  $\mu_{k,m+1} = \theta_{m+1}$ , a large  $\delta_{k,m+1}$  (e.g.,  $2\pi$ ) and a small  $w_{k,m+1}$  (e.g., 0.0001) is pushed on to the stack, or replace the model with least priority if the stack is full.

### 4.3 Discussions

In terms of the above self-learning algorithm, it is worth noting the following questions:

**Why do we model immobility?** Tagwatch models the immobility of a tag instead of its mobility because potential moving states are too many to predefine. The “self-learning” behaves in two aspects: first, any surrounding object will contribute to the building of Gaussian models regardless of their components or shapes. The learned model can be used for future multipath propagation as long as the tags remain in their positions. Second, when a tag moves from one place to another (*i.e.*, state transition), the priorities of its outdated immobility models built for previous positions will be gradually reduced until they are completely removed from the stack.

**When do we learn Gaussian models?** Without need of a particular pre-learning offline, Tagwatch is able to quickly accommodate the influence of a new multipath (*i.e.*, due to changes of environment) online. For example, suppose a new surrounding object comes into the scene, which introduce a new unknown multipath, the stationary tag is mistakenly considered as being in motion in Phase I because none of its learned models can match this new resulted phase value. Then it will be scheduled to be intensively read in the Phase II. The system leverages all recent history readings of the tag including those collected in Phase II, to build its immobility models. In this way, the newly emerged Gaussian model is quickly learned after one cycle (e.g., 3 ~ 5s, see §7). When entering the next cycle, the incoming phase can match the learned model and the tag will be correctly classified as being stationary. Thus, our algorithm does not have a “cold start”.

**How to deal with highly dynamic environment?** As we aforementioned, any motion of a surrounding object moving within a same Fresnel zone creates an equivalent propagation (*i.e.*, distance from the reader to tag passing through the object is equal.), leading to a same Gaussian model. Thus, the number of multipathes are relatively limited. If the system has learned all immobility models incurred by all potential multipathes, it could deal with any interferences from surrounding objects whatever how frequently the environment changes. Thus, the current self-learning algorithm is immune to highly dynamical changes of environment.

<sup>4</sup> $\eta(\cdot)$  refers to Eqn. 9.  $w_{k,m}$ ,  $\mu_{k,m}$  and  $\delta_{k,m}$  respectively denote the weight, expectation, and standard deviation in the  $m^{th}$  iteration of the  $k^{th}$  Gaussian model.

**How to deal with phase jumps?** It is known that the phase value  $\theta = (4\pi d/\lambda + \theta_0) \bmod 2\pi$  where  $\lambda$ ,  $d$  and  $\theta_0$  are wavelength, distance between reader and tag, and initial phase. Due to the operator mod, if the expected value  $\mu$  is around 0 (e.g., 0.02), the measured one  $\tilde{\theta}$  may flip to a value close to  $2\pi$  (e.g.,  $2\pi - 0.01$ ), resulting in  $|\tilde{\theta} - \mu| > \xi\delta$  (e.g.,  $|2\pi - 0.01 - 0.02| = 6.2532 > 3 \times 0.1$ ). Actually, the measured value is very close to the expected. This problem emerges because phase values are represented in the base- $2\pi$  system. To resolve this issue, we would apply the minimum distance for the difference detection in practice. The minimum distance equals  $|\theta_1 - \theta_2|$  if  $|\theta_1 - \theta_2| \leq \pi$ , otherwise equals  $(2\pi - |\theta_1 - \theta_2|)$ , e.g.,  $2\pi - |2\pi - 0.01 - 0.02| = 0.03 < 3 \times 0.1$ .

**How to deal with reading exceptions?** We do not assume all tags are always within the range to the reader throughout. Tags are allowed to come in, go out or be temporarily blocked any time. The system independently creates Gaussian models for each tag. If one tag leaves for a long while, the system will remove its models for saving memory. On contrary, the system immediately creates a Gaussian model stack for any newly emerging tags. If a new tag happens to come in the Phase II, the system will read it in the Phase I of next cycle. There may exist a very extreme case that the tag happens to move into the range every Phase II and move out every Phase I, making the system blind to it. As this tag is definitely a mobile one, we can add its EPC to the configuration file, as described in next section.

## 5 PHASE II: TARGET SCHEDULE

In addition to system-determined mobile tags, Tagwatch also allows user to define tags with significant concerns in a configuration file. These tags will be scheduled for reading regardless of whether they are in motion or stationary. We call these tags, including mobile or concerned tags, *targets* or *target tags*. Then, the question becomes: *how can we exclusively read target tags with existences of a large number of stationary tags?* In this work, we leverage a widely-supported Gen2 command, *i.e.*, `Select`, to selectively read target tags.

### 5.1 Selective Reading

The EPC Gen2 air protocol is the most competitive standard that governs RFID systems worldwide. ISO has ratified it as a part of the ISO/IEC 18000 series. Gen2 specifies an important mandatory command, *i.e.*, `Select`, for *selective reading*. Each inventory round starts with a `Select` command. This command is designed to select a subset of those tags that will participate in the upcoming inventory round. The `Select` command contains six mandatory fields and one optional field. The present study focus on four fields: `MemBank`, `Pointer`, `Length` and `Mask`. These fields work together to indicate a selection condition called *bitmask*. In particular, (1) Gen2 divides the tag memory space into four banks for storing password, EPC, TID and customized data. The `MemBank` field specifies the memory bank to which the `Mask` will be compared with. In our system, the `MemBank` is constantly set to the second bank (*i.e.*, the EPC bank). (2) The `Mask` field contains a bit string for comparison. (3) The `Pointer` field specifies the starting address (*i.e.*, bit number) of the chosen memory bank. (4) The

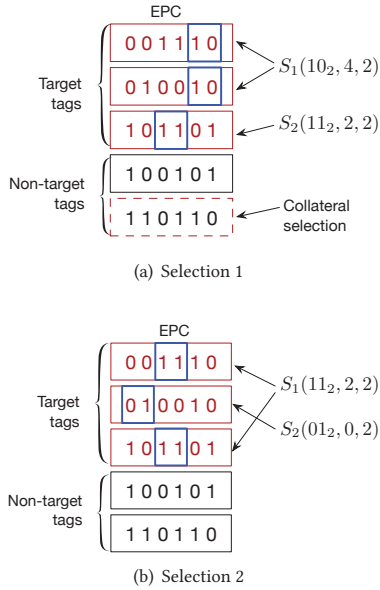


**Fig. 9: An example of bitmask selection.** (a) Bitmasks  $S_1(10_2, 5, 2)$  and  $S_2(11_2, 3, 2)$  completely cover three target tags. However,  $S_1$  mistakenly covers a non-target tag  $110110_2$ . (b) Bitmasks  $S_1(11_2, 3, 2)$  and  $S_2(01_2, 1, 2)$  cover three target tags without non-target tags.

Length field specifies the length of the Mask used for the comparison. For example, if  $\text{MemBank} = 1, \text{Mask} = 0101_2, \text{Pointer} = 2$  and  $\text{Length} = 4$ , then we select the tags whose bit string starting from  $3^{\text{rd}}$  bit and ending at  $(3+4)^{\text{th}}$  bit of the EPC equals  $0101_2$ . The tags are divided into two groups: tags that match the bitmask and tags that do not match the bitmask. We only allow the matching tags to respond the query commands (*i.e.*, *Query*) in the subsequent inventory round.

## 5.2 Bitmask Selection

Suppose that  $n'$  target tags from a total  $n$  tags (*i.e.*,  $n' \leq n$ ) are delivered for selective reading in the second phase. We do not make any assumption on the distribution of the EPCs of target tags as well as those of non-target tags. Any tag can be our target for scheduling. Our task is to seek appropriate bitmasks to cover  $n'$  target tags.

**Challenges.** The search for appropriate bitmasks is non-trivial, and two challenges are encountered. First, a single bitmask is likely unable to cover all target tags in most of time. As shown in Fig. 9(a), no common bitmask can concurrently cover the three target tags. We have to choose a group of bitmasks to cover these targets and then perform multiple rounds of selective reading. For simplicity, we use  $S(m, p, l)$  to denote a bitmask with a Mask  $m$ , a Point  $p$ , and a Length  $l$ . The MemBank field is omitted because this field is fixed to the EPC memory. For example, we select  $S_1(10_2, 4, 2)$  to cover  $001110_2$  and  $010010_2$  whereas  $S_2(11_2, 2, 2)$  for  $101100_2$ , as shown in Fig. 9(a).  $(\dots)_2$  denotes that the number is represented in a binary form. However, such selections are not good because

the selected bitmask  $S_1$  collaterally covers a non-target tag with EPC of  $110110_2$ . Thus, the second challenge is to achieve the optimal selection, which can cover all targets and the least non-targets. For example, the second selection (*i.e.*,  $S_1(11_2, 2, 2)$  and  $S_2(01_2, 0, 2)$ ) shown in Fig. 9(b) is optimal, which covers three targets without any non-targets.

**Naive solution.** The naive method directly uses the  $n'$  EPCs of target tags as  $n'$  bitmasks, such that all target tags are covered without including any non-target tag. Therefore, we must start  $n'$  rounds of inventory rounds with  $n'$  *Select* commands. Each inventory round introduces a start-up cost, which affects IRRs. The optimal strategy is to obtain full coverage on target tags with minimum total time cost. We can consider the naive method as the *worst case*. The cost-effective selection may collaterally involve non-target tags as long as their cost is less than in the worst case. We reduce this problem into the *set cover problem*. Before introducing our algorithm, we describe the set cover problem and subsequently define its relation to the bitmask selection problem.

**Classical set cover optimization problem.** The set cover problem involves selecting a minimum number of sets that contain all the elements in any of the sets in the input. Set cover optimization requires the total cost of the selected sets to be minimal, where each set is assigned a cost. A universal  $\mathcal{U}$  and a family of  $\mathcal{S} = \{S_1, S_2, \dots, S_M\}$  of subset of  $\mathcal{U}$ . Correspondingly, each subset has a weight, denoted by  $\{c_1, c_2, \dots, c_M\}$ . The objective is to find a group of subsets  $\mathcal{I} \subseteq \mathcal{S}$ , such that minimizing  $\sum_{S_i \in \mathcal{I}} c_i$  subjecting to  $\cup_{S_i \in \mathcal{I}} S_i = \mathcal{U}$ .

**Bitmask selection as set covering.** Within our problem domain, the universal set  $\mathcal{U}$  contains the EPCs of  $n'$  target tags, *i.e.*,  $\mathcal{U} = \{\text{EPC}_1, \text{EPC}_2, \dots, \text{EPC}_{n'}\}$ . Each bitmask corresponds to a subset  $\subseteq \mathcal{U}$ , which contains all EPCs covered by the bitmask. Thus, we use a bitmask to denote tag set that it covers. To determine the number of bitmasks (or subsets) do we have, let  $L$  be the bit length of the EPC number (*e.g.*, 96 or 128 bits). The bitmasks can be set with different starting addresses and lengths, hence, we have  $\sum_{l=1}^L (L-l+1)2^l = 2^{L+2} - 2L - 4$  candidate bitmasks in global space. The equation obtains a possible bitmask by sliding a mask from the first position to the last for each length  $l$ . For example, If  $L = 96$ , then  $3.1691 \times 10^{29}$  candidate bitmasks (or subsets) are available, which is too large to be accepted. We only focus on  $n'$  target tags rather than on the entire EPC number space. Therefore, the majority of the subset induced by the global bitmasks are empty, *i.e.*, containing none targets. The candidate bitmask  $S_i$  is selected only when it can cover a target tag. Thus, the actual total number of candidate bitmasks is equal to  $\sum_{l=1}^L (L-l+1)n' = n'L(L+1)/2$ .  $n'$  should be small. Thus, the candidates are controllable. Let  $S_i$  denote a bitmask and the tag set that it covers. Then,  $|S_i|$  is the number of tags covered by this bitmask. The time cost to collect the tags covered by  $S_i$  can be approximated to  $C(|S_i|)$ , as indicated in Definition. 1. Therefore, our problem can be written as the following optimization formula:

$$\begin{aligned} & \text{minimize} && \sum_{S_i \in \mathcal{I}} C(|S_i|) \\ & \text{subject to} && \mathcal{U} \subseteq \bigcup_{S_i \in \mathcal{I}} S_i \end{aligned} \quad (12)$$



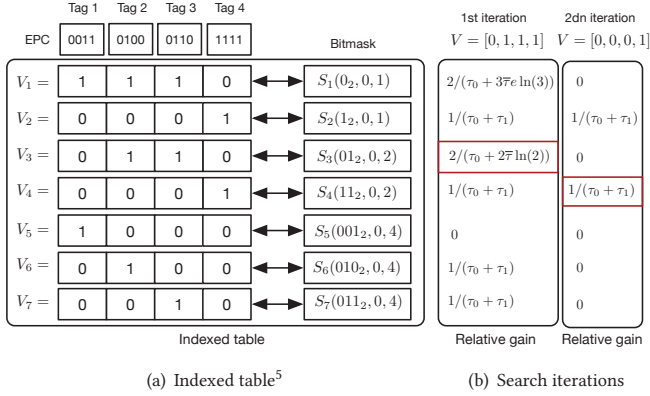


**Fig. 10: An example of bitmask selection.** (a) The pre-built indexed table over four tags in the scene. (b) An execution of the search algorithm, where the input indicator bitmap is equal to  $[0, 1, 1, 1]$ . Finally,  $S_3$  and  $S_4$  are selected.

We reverse the subject condition because the  $S_i$  may contain non-target tags. At first glance, we should select a group of bitmasks purely covering all target tags without non-target tags. Such strategy may not be optimal because it may require excessive bitmasks to achieve its purpose. Consequently, start-up cost is increased, which leads to higher total cost. In addition, the worst cost is always equal to  $C(n')$  when taking  $n'$  inventory rounds that use EPCs of target tags as bitmasks. If the cost of “optimal” selection is higher than  $C(n')$ , we should adopt the worst option.

### 5.3 Bitmask based Schedule

Set cover optimization is an NP-hard problem. Thus we design a greedy algorithm to search for bitmask selection.

**Preprocessing.** Before searching, we build an index table to associate candidate bitmasks with current EPCs, as shown in Fig. 10(a). We arrange all the current tags, including target and non-target tags, based on their EPC values. The left column of the table is an indicator bitmap that shows whether the tag is covered by the right bitmask. For example,  $V_1 = [1, 1, 1, 0]$  because the first three EPCs of the tags are covered by the bitmask of  $S_1(0_2, 0, 1)$ . We traverse all possible bitmasks and generate the corresponding indicator bitmaps that involves all the tags in the scene. We abandon the rows with zero indicators, which do not cover any tag. We also merge the rows whose indicator bitmaps are identical by randomly using one of them because the coverage ranges of these bitmasks are equal. When the indexed table is built, only an incremental update is required, *i.e.*, deleting outgoing tags or adding new ones at the end of the assessment phase.

**Searching for optimal bitmasks.** Tagwatch uses an iterative searching algorithm. An input indicator bitmap  $V$  shows the target tags that should be covered. Each iteration involves the following steps:

<sup>5</sup>This indexed table only considers the bitmasks starting from the first bit due to space limit. The actual table is larger than this one.

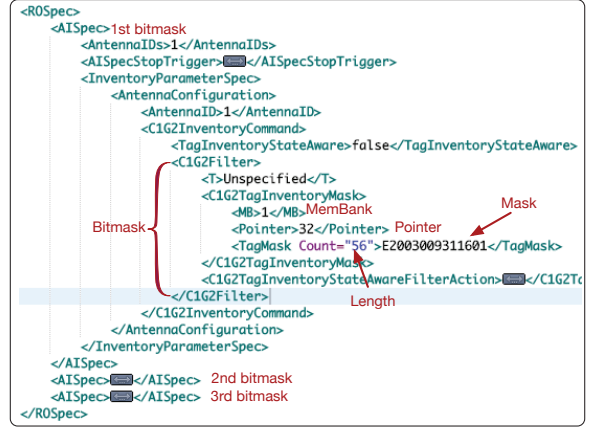


**Fig. 11: An example of ROSpec.** This spec defines three bitmasks for scheduling.

- (Step 1) *The relative gain for each bitmask is calculated.* The relative gain  $R(S_i)$  for the bitmask  $S_i$  is defined by:

$$R(S_i) = \frac{|V_i \& V|}{C(|V_i|)} \quad (13)$$

where  $|V_i \& V|$  is the cardinality of the result of a bitwise “AND” on two bitmaps. It denotes the number of target tags that can be covered using  $S_i$ , and is considered as the absolute gain of  $S_i$ .  $C(|V_i|)$  is the inventory cost if  $S_i$  is used for the selective reading, *i.e.*, inventory cost for reading  $|V_i|$  tags. This cost is considered as the bitmask price.

- (Step 2) *The bitmask with the highest relative gain is selected.* We expect the selected bitmask to identify more target tags with less price (*i.e.*, covering less non-target tags.). A draw can be resolved by random selection.

- (Step 3) *The input indicator bitmap is updated.* Suppose we select the  $j^{th}$  bitmask in Step 2, then  $V = V - (V \& V_j)$ , *i.e.*, the new input bitmap is changed to indicate the target tags that are not covered in this iteration.

- (Step 4) *Return to Step 1 for the next iteration.* The search process is terminated when  $V = 0$ .

A search example is provided in Fig. 10(b) where the original input indicator bitmap  $V = [0, 1, 1, 1]$ , *i.e.*, the last three tags are target whereas the first tag is non-target tag. In the first iteration,  $R(S_1) = 2/(\tau_0 + 3\bar{\tau}e \ln(3))$  because two common “1”s are between  $V$  and  $V_1$  (*i.e.*, gain is equal to 2.), and a total of three tags must be collected (*i.e.*, inventory cost is equal to  $\tau_0 + 3\bar{\tau}e \ln(3)$ ). At the end of the first iteration, we select bitmask  $S_3$  because it has the highest relative gain compared among all the bitmasks. Then, we update  $V = V - (V \& V_3) = [0, 0, 0, 1]$  as the input of the second iteration and select  $S_4$  for the second bitmask. After the second iteration,  $V = 0$  and the search process is terminated.

## 6 IMPLEMENTATION

We adopt the Impinj Speedway R420 reader [2] without making any hardware or software modification. The reader is compatible with EPC Gen2 standard. Four reader antennas with circular polarizations are used to provide a gain of 8dB in two directions. Four

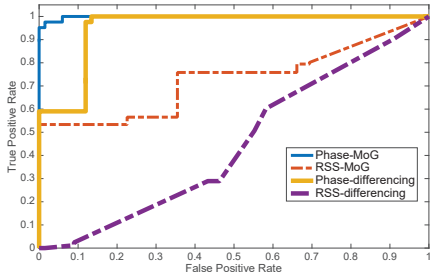


Fig. 12: Detection accuracy.

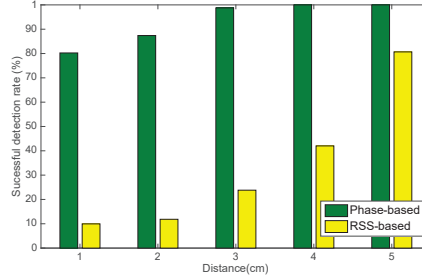


Fig. 13: Detection sensitivity.

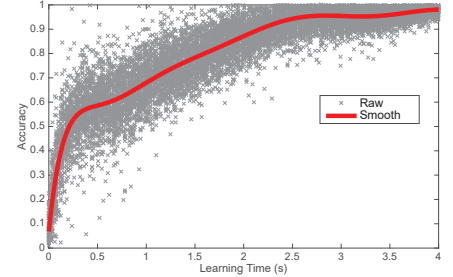


Fig. 14: Learning curve.

types of tags from Alien Corporation [1] are used. We adopt the Impinj LLRP Tool Kit (LTK) to communicate with the reader. LLRP [8] is another protocol specified by EPCglobal that works with Gen2. It is designed to deliver Gen2 parameters from a client to a reader.

**Prototype with LLRP.** LLRP specifies reader operation using ROSpec, which is an XML document that encapsulates parameters of selective reading (e.g., MemBank, Pointer, Mask, Length, etc). Fig. 11 shows a typical ROSpec, where three bitmasks are configured for three selective readings. Each ROSpec is composed of several AISpecs, each of which is used for an antenna setting. An AISpec consists of more than one C1G2Filters. The filters function as the bitmasks. We can set multiple bitmasks by adding multiple C1G2Filters or multiple AISpecs. We adopt the second method by default. After receiving a ROSpec, the reader sequentially starts selective reading.

**Parameter choice.** Tagwatch has several parameters. The key parameters are employed as follows. (1) Reading model: we utilize the least square method to estimate  $\tau_0$  and  $\bar{\tau}$  for the inventory cost (refer to Eqn. 5) by conducting the empirical experiments. Consequently, practical  $\tau_0 = 19ms$  and  $\bar{\tau} = 0.18ms$ . (2) Cycle length: all tags are allowed to be read once in the first phase, thereby the interval of Phase I dynamically depends on the total number of tags. We fix the length of Phase II to 5 seconds. The upper applications can adjust the length of Phase II according to their requirements. (3) For motion detection, the learning rate  $\alpha$ , the number of Gaussian models  $K$  and the threshold  $\xi$  are set to 0.001, 8 and 3.0, respectively, by default.

## 7 EVALUATION

We start a few experiments that provide insight into the operation of the system. We evaluate the performance of the two phases in detail in the following sections.

### 7.1 Evaluation of Phase I

The performance of the motion assessment that occurred in the first phase is first evaluated. We focus on accurately detecting movements with a low false positive rate in a timely manner. To represent false positives, we deploy 100 stationary tags in our office. Approximately 10 individuals work in the room. These people will introduce additional multipath propositions when approaching the tags. We monitor these stationary tags for 48 hours using a reader and collect over 2 million readings. The trace is used as the input

to build the immobility model of each tag and to test for false positive rates. To measure the actual positive rate (i.e., accuracy), we attach a tag on a toy train that moves along an oval track with a radius of 20cm at a constant speed of 0.7m/s. All the readings are considered collected from a mobile tag.

**Detection Accuracy.** Firstly, we investigate the detection accuracy. We present accuracy using the Receiver Operating Characteristic (ROC) curve, which is composed of True Positive Rate (TPR) and False Positive Rate (FPR). We obtain pairs of TPR and FPR by adjusting the detection threshold (e.g.,  $\xi$  in Tagwatch). For comparison, we also use three other methods for baselines. Fig. 12 presents the ROC results, where Phase/RSS-differencing is the naive method that simply compares the incoming RF phase/RSS with the last value. Phase/RSS-MoG utilizes the MoG (Mixture of Gaussian) of phase/RSS to model the immobility of a tag. Consequently, both RF phase-based detection techniques are better than RSS-based methods. In particular, given a FPR of 0.2, Phase-MoG and Phase-differencing achieve 0.99 above TPRs, whereas RSS-MoG and RSS-differencing achieve only 0.53 and 0.12 TPRs, respectively. The RF phase is more sensitive to the motion than RSS. Thus, using phase as a motion indicator is superior to using RSS. However, regardless of which physical indicator (e.g., RF phase or RSS) is used, MoG-based approaches can always control FPRs at a relatively acceptable level compared with differencing. These results show that the multipath effect significantly influences the final received backscatter signals, and MoG effectively depicts this dynamic nature. For example, we can find an appropriate detection threshold to achieve  $\geq 0.95$  TPR while  $\leq 0.1$  FPR using Phase-MoG.

**Detection Sensitivity.** Second, we further study the sensitivity of Tagwatch to motion. Our objective is the timely and accurate monitoring of tag movement, even if its displacement is minimal. During this stage, we move a tag away in a random direction with a displacement ranging from 1cm ~ 5cm. We conduct the experiment 20 times with the same displacement setting. We apply the successful detection rate, i.e., the ratio of the number of successful detections to the total test times as a metric to evaluate sensitivity. Fig. 13 presents the results compared with the results of the RSS-based method. The figure shows that we can successfully detect 87% and 99% of the movement events using RF phase when the tag is moved away from 2cm and 3cm, whereas only 9% and 18% of the events are detected using RSS. Even when the tag is moved away to 5cm ( $\approx 1/4$  wavelength), the RSS-based method achieves a 76% successful rate. In theory, phase value is proportional to twice the

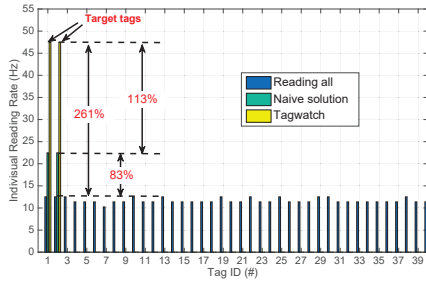


Fig. 15: Schedule feasibility: 2/40

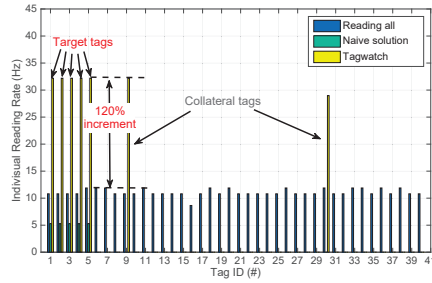


Fig. 16: Scheduling feasibility: 5/40

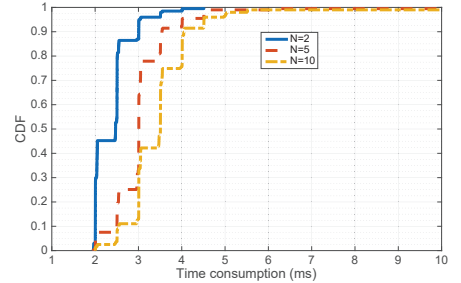


Fig. 17: Schedule cost

distance between the reader and the tag. Thus, when a  $1\text{cm}$  displacement is introduced, an actual change in distance of  $2\text{cm}$  will occur with regard to the RF phase. These characteristics provide a natural amplifier for the RF phase, thereby making it sensitive to movements.

**Learning curve.** Third, we conduct a group of experiments to answer the question: how long does the system need to build a stable Gaussian model? It seems like the system requires a “slow” and “cold” start. In the experiments, we keep a tag stationary and let a person work around. Total one minute readings are collected. We model the tag’s immobility using the first  $10\text{ms}$ ,  $20\text{ms}$ ,  $30\text{ms}$ ,  $\dots$ , and  $10,000\text{ms}$  trace data respectively, and then investigate the detection accuracy using the subsequent  $100\text{ms}$  trace as test data. We say the system conducts a correct detection when the test reading matches one of the immobility Gaussian models. Fig. 14 shows the detection accuracy as a function of time. It suggests that we can achieve 70% and 90% of detection accuracy when fed with  $1.49\text{s}$  trace (*i.e.*, including 67 readings) and  $2.9\text{s}$  trace (*i.e.*, including 130 readings). Therefore, one-cycle readings (*i.e.*,  $5\text{s}$ ) are sufficient to stably create a newly emerging Gaussian model, providing a “quick start” for the self-learning.

## 7.2 Evaluation of Phase II

To understand how Tagwatch operates in the second phase, we deploy a total of  $4 \times 40$  tags with *random* EPCs within the ranges of 4 reader antennas (*i.e.*, each antenna covers 40 tags). In addition, we use the configuration file to directly label target tags to eliminate the influence from the first phase. IRR is used as the metric (*i.e.*, Hz). Each experiment with the same setting is repeated 50 times, and the average result is reported.

**Schedule Feasibility.** To make an intuitive understanding of the scheduling, we show two specific examples in Fig. 15 and Fig. 16, where 2 and 5 tags out of total 40 tags are selected as our targets. In the figure, each tag is associated with three bars that correspond to the IRRs using reading all, Tagwatch, and naive rate-adaptive solution (which simply selects targets’ EPCs as bitmasks). From Fig. 15, we observe that the mean IRRs of the targets (*i.e.*, tag #1 and #2) are approximately  $13\text{Hz}$  in the solution of reading all. By contrast, if Tagwatch is applied, the IRRs of the targets will increase by 261% (*i.e.*, from  $13\text{Hz}$  to  $47\text{Hz}$ ), which is thrice higher than in “all reading”. Naive solution also gives 83% of increment (*i.e.*, from  $13\text{Hz}$  to  $24\text{Hz}$ ). Meanwhile, the IRRs of non-targets drop to zero (note that we focus on the performance of Phase II; thus, the calculation

rate excludes the readings obtained in Phase I.). From Fig. 16, the similar results are observed except two points: first, tag #9 and #30 are collaterally involved into Phase II. Even so, Tagwatch still offers 120% of increment to target tags. Second, the IRRs that naive solution obtained is even lower than that of reading all, because its cost have counteracted its gain. More discussions about IRR will be introduced in the overall evaluation. These two experiments validate that it is completely feasible and effective to perform selective reading through bitmask enabled selection.

**Schedule Cost.** Tagwatch introduces extra time cost on the functions of motion assessment and bitmask selection, *i.e.*, the interval during the end of Phase I and the start of Phase II. This extra time cost may affect the real-time of the system. We slice these extra time consumption from 50,000 cycles, by calculating the time difference between the first reading in Phase II and the last reading in Phase I for each cycle. The CDF of time is illustrated in Fig. 17. We find our additional functions introduce less than  $4\text{ms}$  in the 50% of cycles, and  $6\text{ms}$  in the 90% of cycles. Compared with the 5 seconds of each cycle, such extra consumption can be ignored.

## 7.3 Overall Evaluation

Finally, we present the overall performance of Tagwatch, including two phase readings, by studying the IRR gain and a tracking application.

**IRR Gain.** We evaluate the overall performance through the IRRs of mobile tags. We defined *IRR gain* as the average ratio of IRR obtained by rate-adaptive reading to the IRR obtained by reading all. We present IRR gains with respect to the percent of mobile tags, as shown in Fig. 18. In the figure, we compare two rate-adaptive solutions: one is our Tagwatch, while another is the naive solution that directly uses mobile tags’ EPCs as bitmasks for selective reading. The results of two solutions are plotted in a pair considering a same percent of mobile tags. For each percent, we vary the total number of tags to 50, 100, 200, 300 and 400, and perform 1,000-cycle reading for each setting. All mobile tags are put on a spinning turntable. From the figure, we have the following findings:

- First, when 5% of tags are moving, Tagwatch can improve their IRRs by  $3.2 \times$  in 50% of trials and by  $4 \times$  in 10% of trials. Naive solution can also achieve a gain of  $2.6 \times$  on median. This result suggests that any kind of adaptive-reading solutions can bring efficiency benefits when a few mobile tags exist.
- Second, when 10% of tags are moving, the IRR gain that Tagwatch achieves has a median of  $1.9 \times$  with a standard deviation of

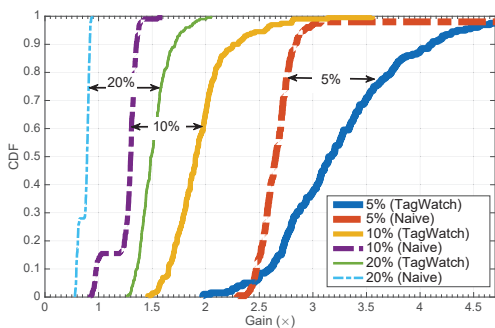


**Fig. 18: IRR gain.** This figure shows the IRR gains of adaptive-reading in terms of different percents of mobile tags.

0.29 $\times$ . In particular, it can achieve a gain of 2.3 $\times$  in 10% of trials. This result suggests that the IRR gain decreases as the percent of mobile tags increases, because more tags participate in the Phase II, making the contention more intense among mobile tags. By contrast, the IRR gain of naive solution is up to 1.5 $\times$ . Clearly the algorithm of bitmask selection used in Tagwatch is superior to broadcasting all.

- Third, when the percent reaches 20%, the IRR gain of Tagwatch is getting close to 1 (e.g., 1.5 $\times$  on average), which means nothing improved. In particular, naive solution has a median gain of 0.8 $\times$ , namely, the actual IRR is lower than that of reading all. Because too much `Select` commands are broadcasted in Phase II, which totally counteracts its gain.

In summary, adaptive reading is completely logical when the mobile tags are a minority (e.g., < 20%). It would provide nearly 4 $\times$  gain without modification on firmware or hardware, which was hardly achieved in prior work. However, as any scheduling will introduce additional cost to start-up and collateral tags, it should notice that the cost may counteract its gains when there are a large number of mobile tags (e.g., > 20%). In such situation, we should simply switch back to the old fashion: reading them one by one.

**Application Study.** Finally, we take the tracking of mobile tags as an application to study the final effect of Tagwatch. In the scene, we deploy four antennas around the surveillance region at the points of ( $\pm 5m$ ,  $\pm 5m$ ). We attach a tag on a mobile toy train and allow it to move along a circular track. The trajectories are recovered using our prior tracking solution [30], namely Differential Augmented Hologram. The experiments are conducted in three different cases: (1 + 0) (# of mobile tags + # of stationary tags), (1 + 2) and (1 + 4). We fix the initial position at a known point to improve comparison. The final results are shown in Fig. 1. Without using Tagwatch, the mean accuracy deteriorates from  $1.8 \pm 0.72cm$  in case (1 + 0) to  $6cm \pm 3.55cm$  in case (1 + 2) and  $10.6 \pm 5.46cm$  in case (1 + 4) due to the channel competition from the stationary tags. By contrast, the mean tracking accuracy remains at  $3.34 \pm 1.42cm$  with rate-adaptive reading even when four interfered stationary tags are placed beside the track. The minimal accuracy loss comes from the apportioned readings in the first phase. Thus, this application study shows that Tagwatch can exactly identify the mobile tag as well as adaptively read it.

## 8 RELATED WORK

A variety of works have been proposed to improve reading rate from two layers. Actually, Tagwatch can work with any of the following designs.

**Physical layer study.** The first group of studies aims to transmit RFID tags in parallel and separate collided transmission in the physical layer. For example, Buzz [26] decodes tag collisions bit by bit. It assumes the linear combination of the *static* channel coefficients of reflecting tags independent of coexisting tags. It cannot apply to moving tags which change their coefficients every second. The linear additional-based scheme proposed in [23] also holds the same assumption. BST [12] enables concurrent transmission by leveraging intra-bit multiplexing of on-off keying signals. It detects signal edges when the distances between consecutive symbols exceed a predefined threshold. BiGroup [21] recovers collisions without modifying COTS tags, but instead, changes the readers. Other designs [3, 5, 16] also recover the collisions of up to two concurrent tags using predefined preambles and stringent tag synchronization. In [14] and [18], orthogonal codes for RN16 are designed for collision recovery.

**Link layer study.** The second group of studies aims to design considerably efficient anti-collision protocols in the link layer [17]. RFID tags rely on the centralized schedule of readers to avoid tag collisions. For example, [19] and [33] propose schemes based on frequency division multiple access and space division multiple access, respectively. Time division multiple access (TDMA) protocols constitute the largest group of anti-collision protocols [4, 7, 15, 28], most of which are variants of DFSA, such as Q-adaptive. Many works have also proposed tree-based protocols [6], which are also a category of TDMA protocols. These protocols operate by splitting responding tags into multiple subsets using a random number generator. In [13] basic tree splitting is presented. In [20] and [6] adaptive binary tree splitting, which dynamically adjusts the tree based on collision history, is proposed.

## 9 CONCLUSION

In this work, we present Tagwatch for the rate-adaptive reading of mobile tags through selective reading. A key innovation is the two-phase reading design, in which mobile tags are read for a relatively long time in the second phase, without competition from stationary tags, thereby improving their IRRs at a significant level. The Tagwatch system has not only been tested and used in practical applications, but will also open a wide range of exciting opportunities.

## Acknowledgments

The research is supported by GRF/ECS (NO. 25222917), NSFC General Program (NO. 61572282), and PolyU Start-up Project (1-ZVJ3). We thank all the reviewers for their valuable comments and helpful suggestions, and particularly thank Prof. Samir R. Das for the shepherding.

## REFERENCES

- [1] 2017. Alien. <http://www.alientechnology.com/>. (2017).
- [2] 2017. Impinj, Inc. <http://www.impinj.com/>. (2017).



- [3] Christoph Angerer, Robert Langwieser, and Markus Rupp. 2010. RFID reader receivers for physical layer collision recovery. *IEEE Transactions on Communications* 58, 12 (2010), 3526–3537.
- [4] ZHEN Bin, Mamoru Kobayashi, and Masashi Shimizu. 2005. Framed ALOHA for multiple RFID objects identification. *IEICE Transactions on Communications* 88, 3 (2005), 991–999.
- [5] Aggelos Bletsas, John Kimionis, Antonis G Dimitriou, and George N Karystinos. 2012. Single-antenna coherent detection of collided FM0 RFID signals. *IEEE Transactions on Communications* 60, 3 (2012), 756–766.
- [6] John Capetanakis. 1979. Tree algorithms for packet broadcast channels. *IEEE Transactions on Information Theory* 25, 5 (1979), 505–515.
- [7] Jae-Ryong Cha and Jae-Hyun Kim. 2005. Novel anti-collision algorithms for fast object identification in RFID system. In *Proc. of IEEE ICPADS*.
- [8] EPCglobal. 2010. Low Level Reader Protocol (LLRP).
- [9] Gary M Gaukler. 2011. Item-level RFID in a retail supply chain with stock-out-based substitution. *IEEE Transactions on Industrial Informatics* 7, 2 (2011), 362–370.
- [10] Mahanth Gowda, Ashutosh Dhekne, Sheng Shen, Romit Roy Choudhury, Lei Yang, Suresh Golwalkar, and Alexander Essanian. 2017. Bringing IoT to Sports Analytics.. In *NSDI* 499–513.
- [11] Hristo D Hristov. 2000. *Fresnal Zones in Wireless Links, Zone Plate Lenses and Antennas*. Artech House, Inc.
- [12] Pan Hu, Pengyu Zhang, and Deepak Ganesan. 2014. Leveraging interleaved signal edges for concurrent backscatter. In *Proc. of ACM HotWireless*.
- [13] Don R Hush and Cliff Wood. 1998. Analysis of tree algorithms for RFID arbitration. In *Proc. of IEEE ISIT*.
- [14] Lei Kang, Kaishun Wu, Jin Zhang, Haoyu Tan, and Lionel Ni. 2012. DDC: A novel scheme to directly decode the collisions in UHF RFID systems. *IEEE Transactions on Parallel and Distributed Systems* 23, 2 (2012), 263–270.
- [15] Girish Khandelwal, Kyoungwan Lee, Aylin Yener, and Semih Serbetli. 2007. ASAP: a MAC protocol for dense and time-constrained RFID systems. *EURASIP Journal on Wireless Communications and Networking* 2007, 2 (2007), 3–3.
- [16] Rushikesh S Khasgiwale, Rohan U Adyanthaya, and Daniel W Engels. 2009. Extracting information from tag collisions. In *Proc. of IEEE RFID*.
- [17] Dheeraj K Klair, Kwan-Wu Chin, and Raad Raad. 2010. A survey and tutorial of RFID anti-collision protocols. *IEEE Communications Surveys & Tutorials* 12, 3 (2010), 400–421.
- [18] Linghe Kong, Liang He, Yu Gu, Min-You Wu, and Tian He. 2014. A parallel identification protocol for RFID systems. In *Proc. of IEEE INFOCOM*.
- [19] Hsin-Chin Liu and Jhen-Peng Ciou. 2009. Performance analysis of multi-carrier RFID systems. In *Proc. of IEEE SPECTS*.
- [20] Jihoon Myung and Wonjun Lee. 2006. Adaptive binary splitting: a RFID tag collision arbitration protocol for tag identification. *Mobile Networks and Applications* 11, 5 (2006), 711–722.
- [21] Jiajue Ou, Mo Li, and Yuanqing Zheng. 2015. Come and be served: Parallel decoding for cots rfid tags. In *Proc. of ACM MobiCom*.
- [22] Longfei Shangguan, Zimu Zhou, Xiaolong Zheng, Lei Yang, Yunhao Liu, and Jinsong Han. 2015. ShopMiner: Mining Customer Shopping Behavior in Physical Clothing Stores with COTS RFID Devices. In *Proc. of ACM SenSys*.
- [23] Dawei Shen, Grace Woo, David P Reed, Andrew B Lippman, and Junyu Wang. 2009. Separation of multiple passive RFID signals using software defined radio. In *Proc. of IEEE RFID*.
- [24] Hao Wang, Daqing Zhang, Junyi Ma, Yasha Wang, Yuxiang Wang, Dan Wu, Tao Gu, and Bing Xie. 2016. Human respiration detection with commodity wifi devices: do user location and body orientation matter?. In *Proc. of ACM UbiComp*.
- [25] Jue Wang, Fadel Adib, Ross Knepper, Dina Katabi, and Daniela Rus. 2013. RF-compass: robot object manipulation using RFIDs. In *Proc. of ACM MobiCom*.
- [26] Jue Wang, Haitham Hassanieh, Dina Katabi, and Piotr Indyk. 2012. Efficient and reliable low-power backscatter networks. In *Proc. of ACM SIGCOMM*.
- [27] Jue Wang, Deepak Vasisht, and Dina Katabi. 2014. RF-IDraw: virtual touch screen in the air using RF signals. In *Proc. of ACM SIGCOMM*.
- [28] Jianwei Wang, Yuping Zhao, and Dong Wang. 2007. A novel fast anti-collision algorithm for rfid systems. In *Proc. of IEEE WiCOM*.
- [29] Teng Wei and Xinyu Zhang. 2016. Gyro in the air: tracking 3D orientation of batteryless internet-of-things. In *Proc. of ACM MobiCom*.
- [30] Lei Yang, Yekui Chen, Xiang-Yang Li, Chaowei Xiao, Mo Li, and Yunhao Liu. 2014. Tagoram: real-time tracking of mobile RFID tags to high precision using COTS devices. In *Proc. of ACM MobiCom*.
- [31] Lei Yang, Yao Li, Qiongzhen Lin, Xiang-Yang Li, and Yunhao Liu. 2016. Making sense of mechanical vibration period with sub-millisecond accuracy using backscatter signals. In *Proc. of ACM MobiCom*.
- [32] Lei Yang, Qiongzhen Lin, Xiangyang Li, Tianci Liu, and Yunhao Liu. 2015. See Through Walls with COTS RFID System!. In *Proc. of ACM MobiCom*.
- [33] Jiexiao Yu, Kaihua Liu, and Ge Yan. 2008. A novel RFID anti-collision algorithm based on SDMA. In *Proc. of IEEE WiCOM*.